NUMERICAL INVESTIGATION OF THE IMPACT OF SHOCK-BOUNDARY-LAYER-INTERACTION ON FAN BLADES

B. Becker*, M. Reyer**, M. Swoboda*
*Rolls-Royce Deutschland Ltd & Co KG
Eschenweg 11, 15827 Blankenfelde-Mahlow
**TU-Berlin, Institut für Luft- und Raumfahrtechnik
Marchstraße 12-14, 10587 Berlin

1. ABSTRACT

The present numerical study was performed to investigate the impact of both the Reynolds number variation and the used turbulence model to capture the boundary layer development on the characteristic of a BR710 fan blade. A one-equation model of Spalart Almaras with an optional semi-empirical transition model of Abu-Ghannam Shaw has been applied. The transition model allows to take the boundary layer development from a laminar to a turbulent behaviour into account. This is of particular importance at low Reynolds numbers and thus high operating altitudes of airplanes when the transition location moves further downstream to the trailing edge. Therefore the interaction between the shock waves of the transonic fan row and the boundary layer leads to a significant change of the characteristic.

The steady numerical studies of the 3-D blade passage have been carried out with the commercial 3-D Navier-Stokes solver NUMECA. Additionally an unsteady calculation has been applied to explain the penalty in efficiency on high operating altitudes.

2. INTRODUCTION

The aim to increase the efficiency of propulsion turbojet engines motivated the designers of fan blades to reduce the pressure losses issued by the viscous effects along the blade surface and the shock losses. Recent airfoil designs are based on so-called transonic laminar profiles leading to a drag reduction of up to 15%. The boundary layer is kept in a laminar shape up to 50% of the cord length by active flow control or by the design of the blade to reach this benefit. This effect is also taken into account within the design process of a fan blade to increase the efficiency of the stage.

In order to take advantage of the effect it is necessary that the design tool provides for the laminar turbulent behaviour of the boundary layer. The transition from a laminar to a turbulent boundary layer has a serious impact on the overall drag, heat transfer and performance of the blade. The influence is increased when the Reynolds number is low.

This is the case for high operating altitudes. For example corporate jets operate at altitudes up to 51kft to get a direct connection to their flight destination. Under these conditions the low density causes high kinetic viscosity and thus the Reynolds number decrease significantly. As a result the transition occurs further downstream on the blade, which leads to an extended length of the laminar boundary layer.

Compared to an airfoil the head shock wave of a blade row enters the blade passage and interacts with the boundary layer of the adjacent blade. Depending on the Reynolds number and the shock angle the boundary layer can be still laminar when the shock impinges the boundary layer. In this case the interaction is stronger than in the turbulent case. The position of the boundary layer transition becomes unstable because of the interaction. This movement of the transition region has to be taken into account within the design process to prevent flutter problems.

3. SHOCK-BOUNDARY-LAYER-INTERACTION

There are general differences between laminar and turbulent shock-boundary-layer interactions. Usually a laminar shock-boundary-layer interaction region is much more sensitive to a large pressure gradient than a turbulent one. Thus the flow can in this case not follow the pressure increase and separates earlier and this causes performance and stability penalties. Furthermore it is well known that the unsteady shock oscillations are much more pronounced in the case of laminar interaction. Knowing the differences, it will be possible to perform a redesign of a fan blade, which is much less sensitive to laminar-turbulent transition effects. To represent the conditions of free flight in a wind tunnel test as realistically as possible, the transition from laminar to turbulent flow is, in most cases, fixed in the proximity of a profile leading edge by means of a transition strip. For traditional transonic airfoils, this assumption was correct because of its geometry and the resulting pressure distribution (front loading which results in strong positive pressure gradient).

In the work of Swoboda and Nitsche [Swoboda and Nitsche (1996)] a direct comparison of flow around a transonic airfoil in fully turbulent (fixed transition) and transitional case is given. They use conventional field measuring techniques and advanced unsteady surface measuring techniques to clarify the differences, which occur during turbulent and transitional shock boundary-layer interactions.

Already when using conventional measuring techniques, large differences between laminar and transition-fixed flow can be observed. In order to illustrate this, the global flow field was measured by means of Laser-2-Focus anemometry in the middle section of an airfoil in a wind tunnel. A CAST7 airfoil was investigated here. The Reynolds number, which is based on profile chord of 0.1m was 1.4 Million. Here, the same shock position that occurs in the two different flow fields was in the focus of interest. As a first and most important result, the free stream Mach numbers differ in the respective cases. As an example, the results of this Mach number

measurement are presented in figure 1 (left) at a shock position of 32% of profile chord. Figure 1 (right) shows the same result for a further downstream located shock position of 47% chord. The differences between free and fixed transition are to be clearly seen. In the case of free transition, the flow accelerates regularly on the suction side into the supersonic region, but slows down as early as in the middle of this region above a front foot of a λ-shock, which is caused by the beginning of the separation bubble. Here, the beginning of the separation bubble has the same effect as a concave edge in the supersonic region. For this reason, the supersonic region is limited by means of a shock that is slightly curved in the upstream direction.

In the case of the fixed transition, the flow is accelerated later on the suction side, and the supersonic region is limited by a more or less vertical (and therefore stronger) shock. Because of greater fluctuations, the supersonic region is also more fully developed above the airfoil in this case. Further downstream of the shock, a slight expansion behind the shock takes place in both cases. This expansion is much more distinct in the case of free transition. In the further course of the experiment, it is to be clearly seen that the flow strongly slows down in the region of the trailing edge in the case of the fixed transition. This is due to a separation on the trailing edge.

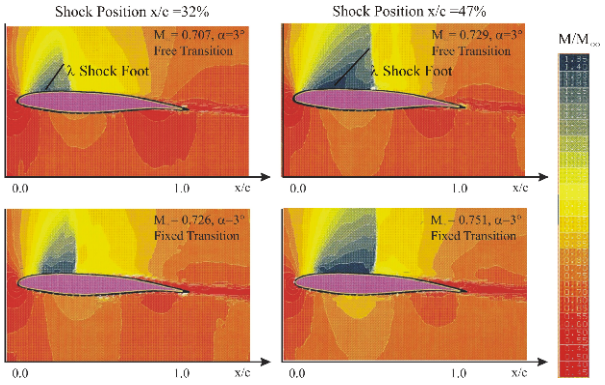

Figure 1: Measured (L2F) Mach number distribution for a CAST 7 airfoil for laminar and fully turbulent boundary layers at two different shock positions

All those effects described above are also valid for turbo machinery flows. To assume an early transition and thus fully turbulent flow is not true in testing turbo machinery because these machines are tested in full scale. The operating range of a turbo machine can vary significantly from take off at atmospheric ambient conditions up to very high altitudes. Consequently, the variation of Reynolds numbers is very high within the operating range of a turbo machine and thus the effects described above are very important and have to be taken into account during the design of turbo machinery components.

4. COMPUTATIONAL METHOD

Within the frame of the presented computations a commercial CFD systems has been employed. FINE™/Turbo, developed by NUMECA Int. S.A (NUMECA [2005]), is a specialized CFD package for all types of turbomachinery applications. The package includes automatic structured grid generation, the flow solver and a post processing software. All program modules are embedded into a turbomachinery specific environment.

The numerical scheme solves the 3D Reynolds-averaged Navier-Stokes equations (RANS) on general structured non-orthogonal multi-block grids. The flexibility of the structured grids is greatly enhanced by use of so-called "Full Non Matching Connections", a technique, which allows to arbitrarily connecting grids block of different grid topologies or point numbers to each other without numerical interpolation losses.

The numerical algorithm incorporated into FINE™/Turbo is an explicit four stage Runge-Kutta scheme (Jameson and Baker [1984]). A variety of convergence acceleration techniques are employed, such as implicit residual smoothing, dual time stepping and a full multigrid algorithm. Space integration is performed using a second order cell-centered finite volume discretization with second and fourth order artificial dissipation. Coarse grid calculations can be carried out in an automatic way on every coarser grid level. A dual time stepping approach was used for the unsteady calculations.

A number of turbulence models are available within FINE™/Turbo. In the scope of the present work the one-equation low Reynolds number model of Spalart and Allmaras (Spalart-Allmaras [1994]) has been chosen, in connection with a transition model. The location of the transition onset and the length of the transition region are based on a semi-empirical approach proposed by Abu-Ghannam and Shaw [1980].

5. TRANSITION MODEL

For the simulations in the present work the one-equation turbulence model of Spalart and Allmaras (Spalart and Allmaras, [1992]) was used in combination with the transition model of Abu-Gahnnam Shaw.

The one-equation turbulence model of Spalart-Allmaras models writes as:

$$\frac{D\tilde{\nu}}{Dt} = c_{b1}[1-f_{t2}]\tilde{S}\tilde{\nu} + \frac{1}{\sigma}[\nabla.((\nu+\tilde{\nu})\nabla\tilde{\nu}) + c_{b2}(\nabla\tilde{\nu})^2] - [c_{w1}f_w - \frac{c_{b1}}{\kappa^2}f_{t2}]\left[\frac{\tilde{\nu}}{d}\right]^2 + f_{t1}\Delta U^2 \quad (0.1)$$

where ν is the molecular kinematic viscosity and $\tilde{\nu}$ denotes the turbulent working variable (Spalart and Allmaras, [1992]). The f_{t2} term has been introduced by Spalart and Allmaras in order to alter the production term so that a zero value of $\tilde{\nu}$ becomes a stable solution in the laminar region. This term writes:

$$f_{t2} = c_{t3}\exp(-c_{t4}\chi^2) \quad (0.2)$$

where $\chi = \tilde{\nu}/\nu$.

The last term on the right-hand side of equation (1) is the "trip" term, which promotes turbulence. It depends on ΔU, which is the norm of the difference between the velocity at the trip point and that at the field point considered, and on the f_{t1} function. The trip function writes:

$$f_{t1} = c_{t1} g_t \exp\left(-c_{t2} \frac{\omega_t^2}{\Delta U^2} [d^2 + g_t d_t^2] \right) \quad (0.3)$$

ω_t denotes the vorticity at the closest transition point, whereas d_t is the distance to this point. d is the distance to the solid wall. The g_t factor allows the shape of the ellipse to depend on the grid spacing along the wall at the trip: Δx_t. It is defined as:

$$g_t = \min\left(0.1, \frac{\Delta U}{\omega_t \Delta x_t} \right) \quad (0.4)$$

The model constants in this formulation are $c_{t1} = 10$, $c_{t2} = 2$, $c_{t3} = 1.2$, and $c_{t4} = 0.5$.

In order to apply this model in unsteady mode, re-laminarisation has to be allowed. One option is to introduce a so-called intermittency, Γ. It is defined as the fraction of time during which the flow over any point on a surface is turbulent. It should be zero in the laminar boundary layer and unity in a fully developed turbulent boundary layer. The intermittency is used to multiply the production term. For the Spalart-Allmaras turbulence model this leads to:

$$\tilde{S} = \Gamma \tilde{S} \quad (0.5)$$

Free-stream wakes (with only a weak production term) will not be affected by the intermittency. A laminar boundary layer will be preserved upstream of the transition location and turbulence could freely develop thereafter. As a default the intermittency is zero before transition and one after the transition onset (binary behaviour). Transition was therefore triggered, unnaturally, in an on-off manner. In order to gain more insight about the effect of intermittency Hildebrandt et. al (Hildebrandt et. al [2005]) have performed calculations with an intermittency distribution according to Dhawan & Narasimha (1958). There are only small deviations compared to the non-intermittent results without an intermittency distribution. The transition onset is moved only slightly downstream in the case of a calculation with an intermittency distribution.

6. INVESTIGATED FAN BLADE

Most calculations were carried out on an early preliminary design of a BR710 fan blade. The BR710 engine, which powers a number of corporate jets, is equipped with a fan of 48inch diameter. The jets equipped with this engine are designed to fly at very high altitude of up to 51.000 ft. The atmospheric conditions at this altitude result in very low Reynolds numbers. To explore the differences between ambient sea level conditions and the flight at high altitude the fan blade was calculated at both conditions. The reduced rotational speed was kept constant in order to ensure comparable inlet conditions in terms of the Mach number. Below, the Reynolds numbers are depicted:

BR710 Fan	**Sea Level:**	$\mathrm{Re}_{sea} = 2.3 \cdot 10^6$
BR710 Fan	**51kft Altitude:**	$\mathrm{Re}_{alt} = 5.06 \cdot 10^5$

7. NUMERICAL GRID

The mesh is a structured multi-block topology consisting of a total of 9 mesh blocks leading to an overall grid size of approximately 1.6 million grid points.

Figure 2 shows the overall computational domain and the respective calculated passage. Further details of the grid are shown in figure 3 at mid span position. The tip clearance is resolved quite fine with 17 radial grid points to resolve the tip clearance vortex flow.

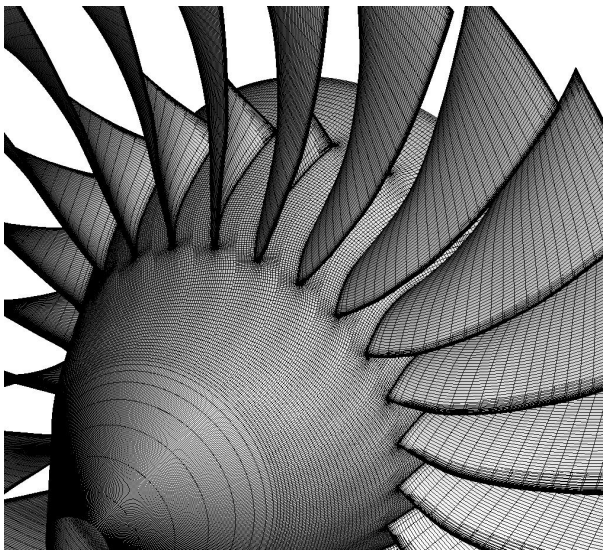

Figure 2: BR710 fan blade coarse grid (skip=2), repetition.

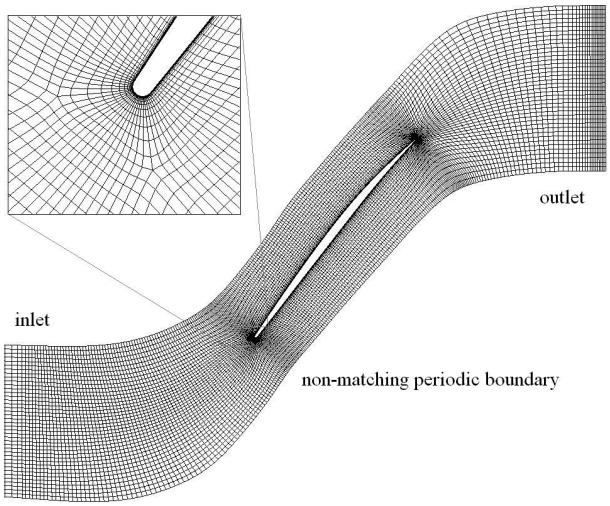

Figure 3: Grid at mid span in blade to blade view and boundary conditions fort he computational domain

The Spalart-Allmaras turbulence model is used in a low-Reynolds formulation without wall functions requiring a fine mesh resolution to ensure at least a few cells inside the lami-

nar sublayer. Consequently, the non-dimensional wall distance should be in the range of values within the viscous sublayer verified by figure 4 (rotor at midspan).

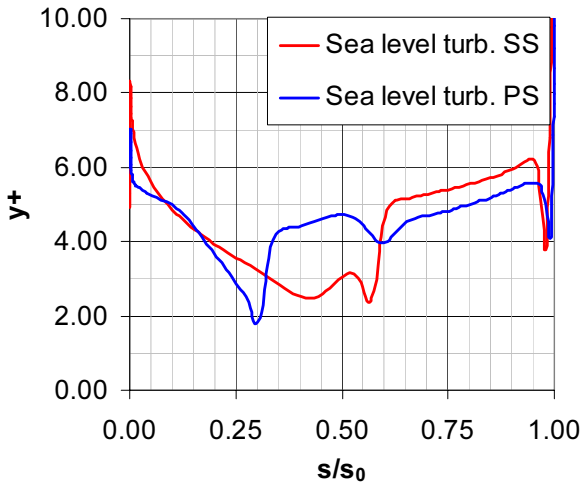

Figure 4: y+ values in the first cell above the blade surface on the suction side and pressure side

Since the y^+-values are directly correlated with the wall shear stress, a transition location can be observed on these values, because higher levels of wall shear stress result in higher y^+-values. On the suction side the on-set of transition can be observed at ~s/s_0= 0.6, whereas the transition on the pressure side is located at ~s/s_0= 0.3

The calculations have been carried out on a single processor INTEL 2.6 GHz processor. Computational time for one operation point was in the order of 6h, typically leading to a reduction in residual of 4 orders of magnitude.

8. BOUNDARY CONDITIONS

In table 1 the boundary conditions for both calculations are listed. Total pressure, total temperature, flow angle and turbulent intensity are prescribed at the inlet. The flow enters the calculation domain in axial direction. For the calculation of the characteristics (pressure ratio and efficiency versus mass flow) the exit pressure was varied. For that reason a simple radial equilibrium was applied for every of the applied pressures at the exit.

		sea level	altitude 51kft
Inlet	p_{t1} T_{t1} ν_{t1}	101350 Pa 288 K 10e-4 m^2/s	20208 Pa 227 K 10e-4 m^2/s
Outlet	p_2	86000 … 108000 Pa	17150 … 23000 Pa

Tab.1: Boundary Conditions

9. RESULTS AND COMPARISON

Steady calculations with a fully turbulent and a transitional treatment of the boundary layer for two different operating altitudes are compared in the first subsection. An unsteady calculation with transition model for an altitude case was added because a significant change in the characteristic of the fan was found in the steady calculations. The results of the unsteady part of the investigations are discussed in the second subsection.

9.1. Steady Investigation

Four compressor characteristics were calculated by increasing the backpressure step by step at the outlet of the computational domain. Depending on the usage of the transition model and the operating conditions at sea level and altitude the characteristic of the fan changes (see figures 5 and 6).

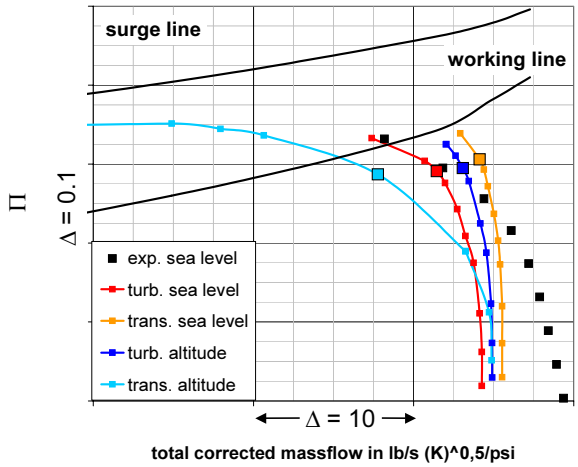

Figure 5: Fan characteristic pressure ratio over reduced mass flow

Both the pressure ratio and the efficiency is increased by switching from the turbulent boundary layer calculation to the transition model at sea level conditions whilst the behaviour is vice versa for the altitude operating conditions. The transition model calculates smaller pressure ratios and poorer efficiencies near the working line at high altitudes and low Reynolds numbers. It should be mentioned that the calculation for the flight case in high altitudes matches the behaviour of the experimental results best even though the values are under predicted.

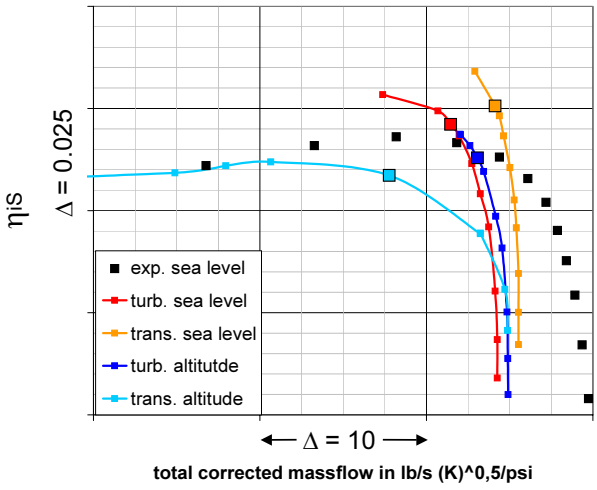

Figure 6: Fan characteristic adiabatic efficiency

The turbulent calculation of the boundary layer is less influenced by the operating altitude and therefore by the Reynolds

number. Because the development of the boundary layer is not taken into account by the turbulence model, the results are less dependent on the Reynolds number.

To investigate the effect of the transition on the fan characteristic near the working line (highlighted points in figures 5 and 6), the shear stress coefficients cf number along the blade surface at 93% span are compared to each other in figures 7 and 8.

It is obvious that the choice of the transition model leads to a significant change in the wall stress distribution for both operating altitudes. The reduced shear stress at the first section of the blade especially for the sea level case is due to the laminar behaviour of the boundary layer. The cf values of the calculations with the transition model approximate to the turbulent solutions after the shock wakes impinge at the positions s/s0=0.2 at the pressure side and s/s0=0.5 at the suction side.

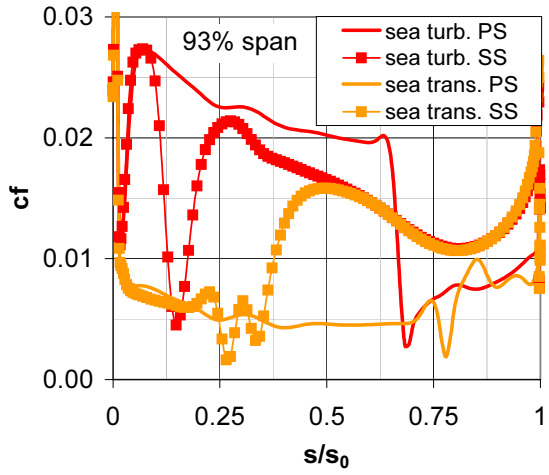

Figure 7: cf at fan blade surface at 93% span for sea level conditions

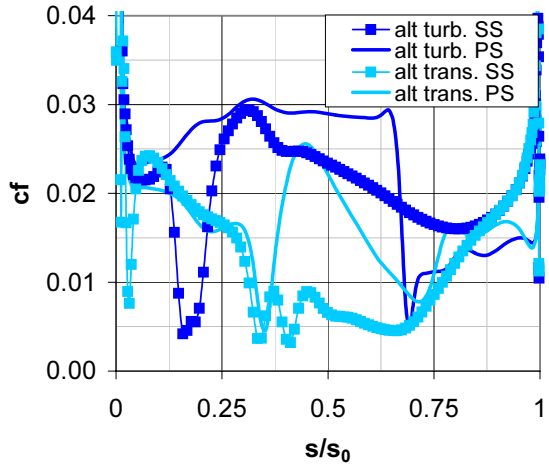

Figure 8: cf at fan blade surface at 93% span for altitude conditions

Further downstream where the boundary layer is turbulent in both calculations with the turbulence model and the transition model the cf values are in good agreement for sea level conditions. This is not the case for the operating altitude of 51kft where the cf distribution shows a peak after the shock attaches the suction side of the blade.

Close to the shock position the transition from laminar to turbulent boundary layer occurs. It is assumed that the boundary layer transition is triggered by the shock. The existence of the laminar flow, represented by the blue colour, at the inlet of the blade is shown in figure 9 for the sea level and the altitude case.

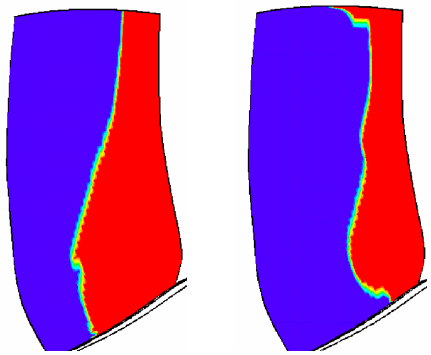

Figure 9: Intermittency at suction side for sea level (left) and altitude (right), blue laminar, red turbulent boundary layer treatment

Even for the high Reynolds number in the sea level case the boundary layer keeps laminar in the first part of the blade. The transition line moves downstream for the altitude conditions, as can be seen in the right contour plot in figure 9. Due to the lower Reynolds number the laminar boundary layer is extended further towards the trailing edge.

The shock position is shown in the plot of the relative Mach number in the blade to blade section at 93% span in Figure 10.

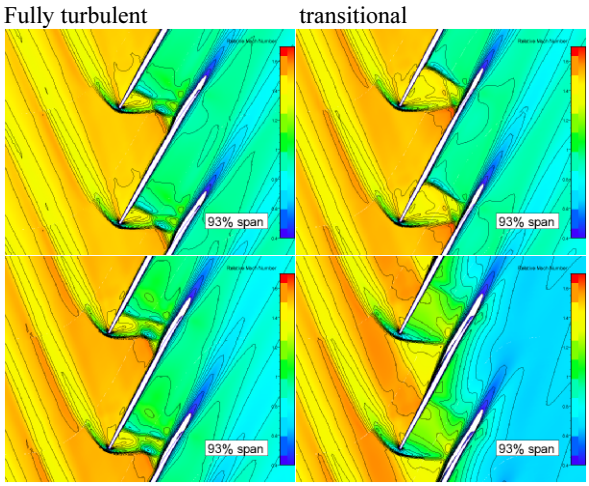

Figure 10: Relative Mach number at 93% span (from upper left to bottom right: turb. sea level, trans. sea level, turb. altitude, trans. altitude)

The location of the shock is significantly changed when the transition model is used. Further more the passage blocking moves downstream and increases the regions where boundary layer shock interactions take place. As mentioned before the

laminar boundary layer interacts more sensitive with the shock than the turbulent boundary layer. Therefore the interaction region becomes bigger in the calculation with the transition model and the passage blocking moves further downstream. Further more the boundary layer thickness develops slower in the transition model calculations due to the consideration of the laminar boundary layer. Because of the thinner boundary layer at the passage inlet the minimum channel height is reached later than in the fully turbulent calculation. Especially in the altitude case with low Reynolds number the passage shock is changed close to the suction side.

The static pressure was related to the total pressure at the stagnation point of the fan blade and was plotted for all investigated parameters to ascertain the differences in the characteristic of the fan stage (see figures 11 and 12). The additional black lines in the plots represent the pressure p* where speed of sound is reached.

The shock is located at the intersection points of the pressure lines with the constant p*=0.528 line. The shock attaches the blade surfaces later when the transition model is used. This corresponds to the contour plots of the relative Mach number wherein the passage shock is located further downstream.

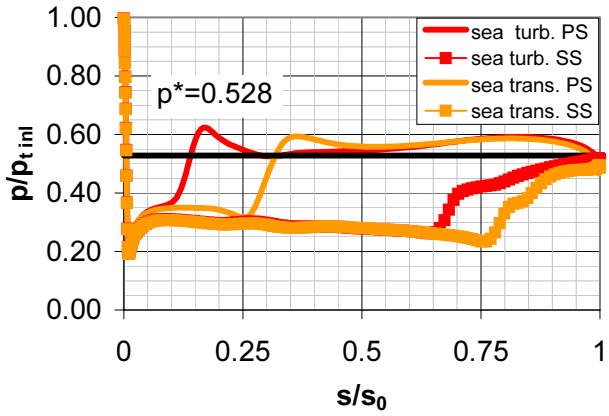

Figure 11: Static pressure distribution on the fan blade surface at 93% span for sea level conditions

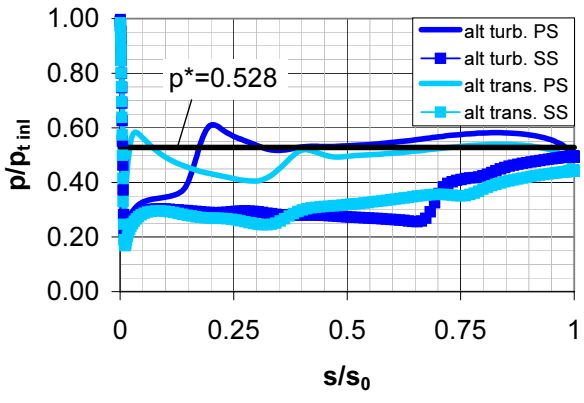

Figure 12: Static pressure distribution on the fan blade surface at 93% for altitude conditions

The flow especially in the tip region of the blade is more sensitive at low Reynolds numbers in the transitional simulation. This was also observed by Kügeler et al. (Kügeler , Weber, Lisiewicz [2001]) where a separation bubble and a lambda-type shock on the suction side of the DLR-TSG-97-cascade transonic profile was more pronounced in the transitional computation case.

The separation bubbles are identified by the iso lines in the vector plot of the tangential component of the velocity in figure 13. Whilst the separation starts for the turbulent calculations more or less at the same point at 93% span, the behaviour in the transitional computation is completely different. In the sea level case the separation moves further downstream compared to the turbulent calculation. Under the altitude conditions the separation occurs significantly earlier. More than 60% of the cord length of the blade the flow is separated from the suction side surface (see also figure 12). Therefore the blade to blade passage is blocked by the thickened boundary layer at the passage exit. This leads to the reduced mass flow in the fan characteristic at high altitude conditions and a penalty in the efficiency (see figure 5).

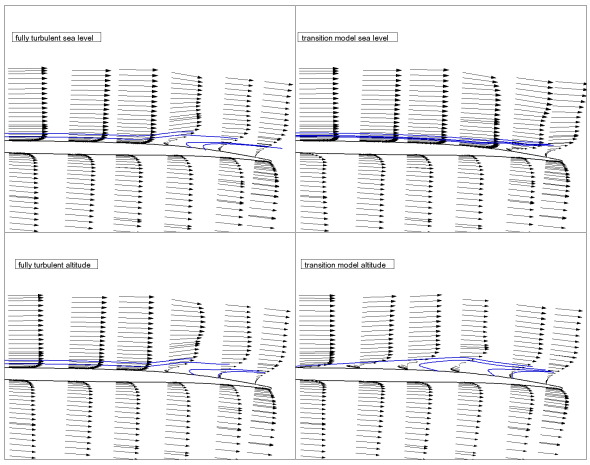

Figure 13: Vector plots and iso lines at the trailing edge of the fan blade (from upper left to bottom right: turb. sea level, trans. sea level, turb. altitude, trans. altitude)

9.2. Unsteady Investigation

Based on the results of the steady simulations, which demonstrate the time averaged impact of the described effects, additional unsteady simulations were conducted to further investigate the dynamic behaviour. A detailed analysis of the unsteady results was performed to gain insights into the prevailing flow conditions, especially with regard to a further development of the fan to increase the efficiency and to guarantee a robust operating behaviour. The characteristic parameters describing the periodic, time-dependent operating behaviour of the BR710 fan are given by the rotation speed and the number of blades. For the simulated operating point this results in a Strouhal-number of Sr=0.109 using the rotation speed and a Strouhal-number of Sr=2,609 using the number of blades.

Figure 14 displays these parameters. One section (alternation of white and grey) and one revolution (alternation of blue and transparent) are accentuated by different colours.

In contrast to the fluctuations in the mass flow at the inlet and outlet of the computational domain, which are also shown in figure 14, the frequencies of the time-dependent flow behav-

iour proved to be no multiple of the typical temporal parameters of the fan. From a Fourier-Analysis of these mass flow fluctuations, which are in-phase, a dominant Strouhal-number of Sr=0.8 can be found. This corresponds to exactly 125 iterations of the time steps, which are used in the simulations. The cause of this very dynamic flow behaviour lies within the interaction of shock and boundary layer and is also influenced by the familiar phenomena occurring for the flow through the clearance at the top of the fan's blades. For a better understanding of this behaviour, figure 15 displays four images with a constant time interval.

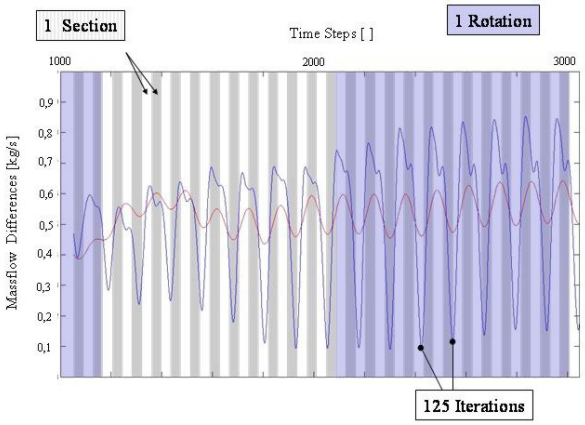

Figure 14: Graphical representation of the mass flows at the inlet and outlet of the computational domain to characterize the time-dependent operating behaviour of the flow in the fan

On the surface of the blade, isolines of the friction coefficient are shown, whereas the relative Mach-number distribution is displayed for different planes inside the section. Starting at the lower right image and continuing clockwise, a vortex near the wall at the trailing edge can be seen, which moves downstream and away from the wall, is weakened and advances to the wake. This dynamic behaviour is caused by the time dependent flow through the tip clearance, which in turn is decisively governed by the shock-boundary layer-configuration on the suction side of the blade.

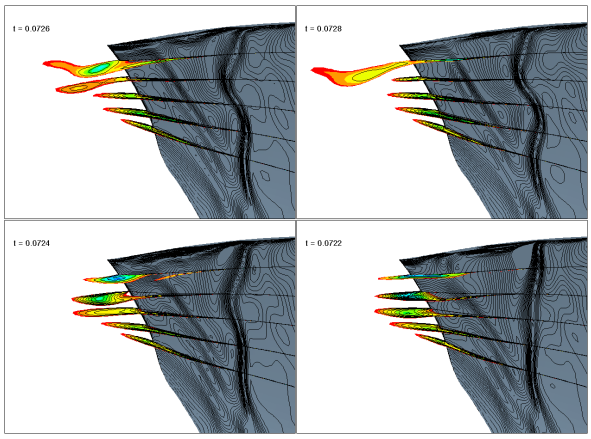

Figure 15: Distribution of cf on the suction side and relative Mach number in passage cutting planes in the tip region of the blade at different times t_n.

These time-dependent fluctuations of the shock configuration trigger the periodic fluctuations in the mass flows at the inlet and even more at the outlet of the computational domain.

These strong fluctuations in the mass flows also entail load changes for the resulting forces, which in turn can cause flutter for critical operating points. By means of the results from these numerical simulations, preventive measures can be developed.

10. SUMMARY AND OUTLOOK

The present paper describes the complex impact of laminar-turbulent transition to shock boundary layer interactions. The physical effects in the interaction region are described in detail on the basis of surface pressure and laser measurements carried out on a transonic airfoil profile CAST 7. At the same free stream Mach number, the position of a shock on the airfoil is always located further downstream in the case of free transition (i.e. laminar flow in front of the shock). Also, a laminar separation bubble develops far in front of the shock in the case of transitional shock boundary-layer interaction.

To assess these effects on a transonic fan blade a CFD package (NUMECA Int.) with a transition criterion was used. The transition model according to Abu-Ghanam and Show, which is described in detail was implemented in the Spalart-Allmaras one-equation turbulence model. The BR710-fan was calculated in different operating conditions, i.e. at sea level altitude with high Reynolds number and in very high altitude, which represents low level of Reynolds number. For both cases fully turbulent and transitional computations were carried out for comparison reasons. Especially at low Reynolds number i.e. high altitude, the differences in the blade characteristics (pressure ratio and efficiency versus mass flow) are considerable. These are mainly caused by significantly different shock positions in both cases, which are caused by different throttling of the passage due to different boundary layer thickness. Again, the shock is located much further downstream in the passage for the case of transitional flow. In the tip region of the blade the transition model implies a boundary layer separation, which is more pronounced than in the fully turbulent calculation. Therefore an unsteady investigation of the fan blade for the altitude operating conditions with transition model was performed.

It was found that the tip flow separates with a Strouhal-number of Sr=0.8, which is not related to the blade passing frequency. The unsteady tip vortex interacts with the shock and thus with the transition location. As a result the periodic separating vortex decreases the efficiency and the mass flow through the machine.

Having these effects in mind it will be possible to design future fan blades which account for the real transitional shock boundary layer effects, especially at low Reynolds number operations.

11. REFERENCES

Abu-Ghanam, B., Shaw, R.: Natural transition of boundary layers. The effects of turbulence, pressure gradient and flow history, J.of Mech. Engeneering Science, Vol.22, pp. 213-228, 1980

Dhawan, S., Narasimha, R.: Some properties of Boundary Layer During the Transition from Laminar to Turbulent Flow Motion, J. of Fluid Mechanics, Vol.3, pp. 418-436, 1958

Hildebrandt, Th., Swoboda, M., Lorrain, E.: Steady and Unsteady Transitional 3D Navier-Stokes Calculation of a 1,5-Stage Axial Low Speed Compressor, Proceedings of 17th International Symposium on Airbreathing Engines, 4.-9. Sept. 2005, Munich, Germany, 2005

Kügeler, E., Weber, A., Lisiewicz, S.: Combination of a Transition Model with a Two-Equation Turbulence Model and Comparison with Experimental Results, Proceedings 4th European Turbomachinery Conference, Florence, Italy, Paper No. ATI-CST-076/01, 2001

Spalart, P.R., Allmaras, S.R.: A one-equation turbulence model for aerodynamic flows, AIAA-92-0439, 1992

Swoboda, M., Nitsche, W.: Shock Boundary-Layer Interaction on Transonic Airfoils for Laminar and Turbulent Flow, Journal of Aircraft, Volume 33, Number 1, Jan.-Feb. 1996